Fluid transfer and vein thickness distribution in high and low temperature hydrothermal systems at shallow crustal level in southern Tuscany (Italy)

Francesco Mazzarini[1,*], Giovanni Ruggeri[2], Ilaria Isola[1], Chiara Boschi[3], Andrea Dini[3], Giovanni Musumeci[1,4], Sergio Rocchi[4]

[1] *Istituto Nazionale di Geofisica e Vulcanologia, Sezione di Pisa, Pisa, Italy*

[2] *Istituto di Geoscienze e Georisorse, CNR, Firenze, Italy*

[3] *Istituto di Geoscienze e Georisorse, CNR, Pisa, Italy*

[4] *Università di Pisa, Dipartimento di Scienze della Terra, Pisa, Italy*

Article history
Received November 22, 2012; accepted May 6, 2014.
Subject classification:
Hydrothermal systems, Vein thickness distribution, Transmissivity, Tuscany.

ABSTRACT

Geometric analysis of vein systems hosted in upper crustal rocks and developed in high and low temperature hydrothermal systems is presented. The high temperature hydrothermal system consists of tourmaline-rich veins hosted within the contact aureole of the upper Miocene Porto Azzurro pluton in the eastern Elba Island. The low temperature hydrothermal system consists of calcite-rich veins hosted within the Oligocene sandstones of the Tuscan Nappe, exposed along the coast in southern Tuscany. Vein thickness distribution is here used as proxy for inferring some hydraulic properties (transmissivity) of the fluid circulation at the time of veins' formation. We derive estimations of average thickness of veins by using the observed distributions. In the case of power law thickness distributions, the lower the scaling exponent of the distribution the higher the overall transmissivity. Indeed, power law distributions characterised by high scaling exponents have transmissivity three order of magnitude lower than negative exponential thickness distribution. Simple observations of vein thickness may thus provides some clues on the transmissivity in hydrothermal systems.

1. Introduction

Focused fluids in the crust are involved in metamorphic, magmatic, hydrothermal, and ore body formation processes; they exploit the existing fracture network or generate new fractures. Fluid circulation in fractures is peculiar of fluid–rock interaction during regional metamorphism and it occurs also in geothermal systems where it is supposed to control most of the fluid flow, occasionally representing the most productive reservoirs [e.g. Hanson 1995, Oliver 1996, Bertini et al. 2006]. During contact metamorphism, fluid production from magma and wall rocks, thermal expansion of fluid, thermal and chemical buoyancy, topography, and deformation of rocks all interact to drive fluid circulation [Hanson 1995, Oliver 1996, Cui et al. 2001].

Simulation of hydrocarbon or geothermal reservoirs needs to model fracture network taking into account: i) the hierarchical arrangement of networks of different fracture typologies (i.e. stratabound and non-stratabound fractures; Odling et al. [1999], Ortega et al. [2006]), ad ii) the hydraulic properties of actual fracture network as fracture connectivity, permeability and transmissivity [Darcel et al. 2003, Guerriero 2012, Guerriero et al. 2011, 2013]. Greater depths favor the development of non-stratabound fracture systems whereas stratabound systems are expected to develop mainly at very shallow crustal levels [Odling et al. 1999].

Field structural data are used to define natural analogues of reservoirs by measuring along sample lines fracture orientation and morphology, crosscutting relationships, composition and texture of fracture fill, and mechanical-layer thickness of the beds.

Opening displacement (or kinematic aperture) of each fracture, intercepted by a fracture set–perpendicular scan line, was also recorded [e.g., Ortega et al. 2006, Guerriero et al. 2013]. This approach uses surface data of actual fracture network to simulate fracture network behavior at depth.

Mineral filled fractures (veins) record fluid paths and composition at the time and at the depth of their formation. Precipitation of minerals occurs when the

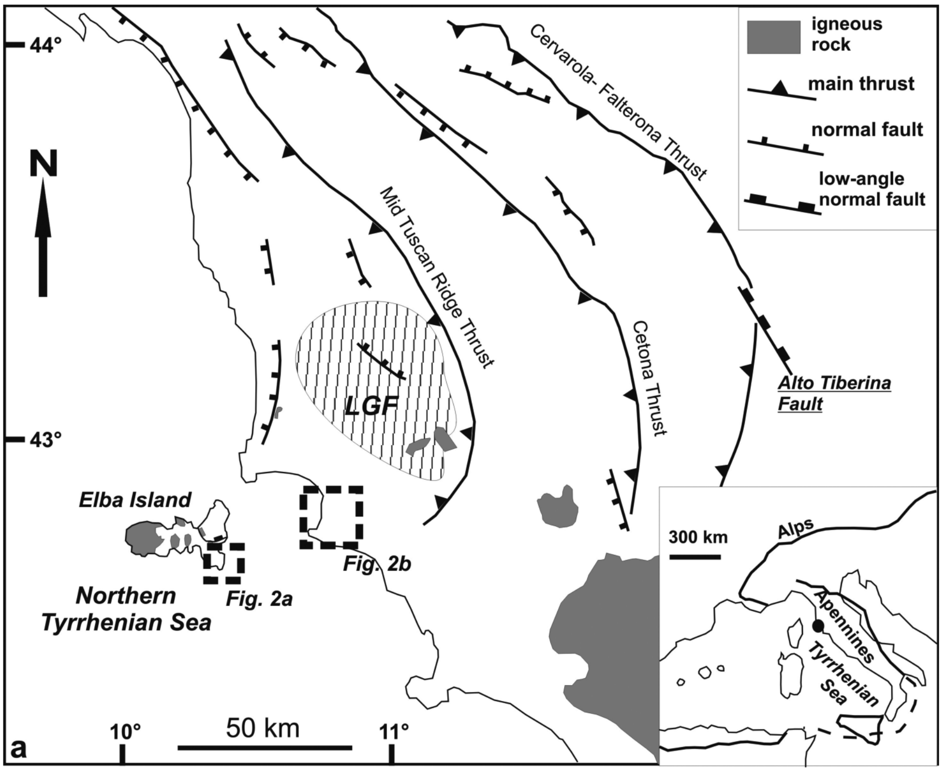

Figure 1. Sketch map of geological setting of studied examples (black dashed boxes), LGF: Larderello Geothermal Field. Dot in the inset is the location of this study.

fluid pressure drops after a phase of an intense increase [Bons 2001, Cox et al. 2001]. Veins are extension fractures that are filled with mineral deposits, and can be used to study the geometric and hydraulic features of fracture networks in the crust [e.g. Vermilye and Scholz 1995, Johnston and McCaffrey 1996, McCaffrey and Johnston 1996, Roberts et al. 1999, Bonnet et al. 2001]. Geometric features of veins and their spatial distribution may thus be used to define parameters relating to fluid pressure, stress state and hydraulic connectivity between vein systems [e.g. Mazzarini and Isola 2007]. Full characterization of vein systems requires knowledge on veins attitude, size (length, height, aperture), spatial distribution (spacing, density) and the composition of filling minerals. The vein aperture is a geometric parameter straightforwardly linked to fluid circulation. Indeed, the hydraulic transmissivity of a fracture (an open void, i.e. an high permeability zone) is the permeability integral over the fracture aperture [Hsieh 1998]. According to Witherspoon et al. [1980] hydraulic transmissivity of a fracture is proportional to the cubic power of the fracture aperture at the time of fluid circulation. The thickness of the veins (w) is thus a good proxy for the fracture hydraulic aperture. Therefore, veins thickness distribution could give information on the overall hydraulic transmissivity of the veins system.

We present two examples of hydrothermal fluid circulation in veins network; the first one is characterized by high temperature fluids circulating within a contact aureole (The Calamita hydrothermal system), the second one is characterized by low temperature fluids circulating within Oligocene sandstones (The Scarlino hydrothermal system). Based on the analysis of the thickness distribution of veins in both the hydrothermal systems, we make inferences on the transmissivity of vein networks in order to investigate the conductance of vein systems.

2. Case study

The studied hydrothermal systems are located in southern Tuscany, in the inner sector of the Apennines belt (Figure 1), which was formed by continental collision between the European margin and the Adria promontory after the closure of the Ligurian-Piedmont ocean [Boccaletti et al. 1971]. The belt architecture resulted from late Oligocene – early Miocene (Burdigalian) eastward stacking of tectonic units scraped off the Tethyan oceanic crust (Ligurian units) and the Adria continental margin (Tuscan Nappe and Tuscan Metamorphic Complex). Since the late Miocene, the innermost portion (Tyrrhenian side) of the northern Apennines region has been affected by subduction-related calc-alkaline magmatism (Tuscan Magmatic Province; Serri et al. [1993], Rosenbaum et al. [2008]) characterized by mainly intrusive rocks, which extend from the northern Tyrrhenian Sea (Capraia, Giglio, Montecristo and Elba islands) to the inner portion of the northern Apennines. Magmatism gets younger

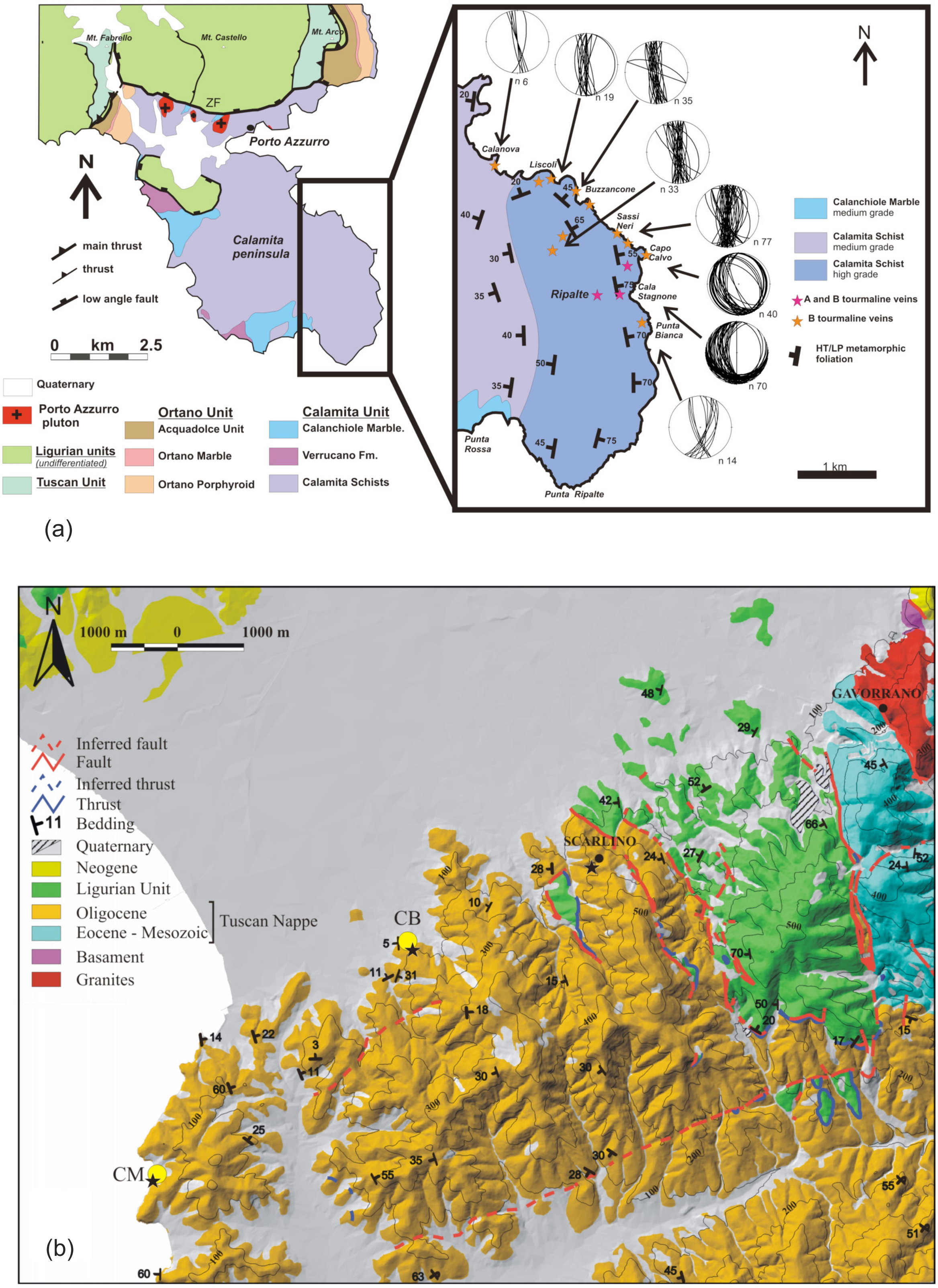

Figure 2. (a) Eastern Elba island geology and geological map of the Calamita peninsula with location of stops where tourmaline veins have been studied (after Mazzarini et al. [2011]). Lower hemisphere stereo plots of measured veins at each sites, n is the number of measured veins. (b) Scarlino area geological map with position of Cava Botrona (CB) and Cala Martina (CM) sites (after Mazzarini et al. [2010]).

eastwards with ages spanning from 8.4 (Capraia and Elba islands) to ~0.3 Ma (Mt. Amiata). It was coeval with the opening of the Tyrrhenian Sea as a back-arc basin as a consequence of slab roll-back of the westward subducting Adria lithosphere [Malinverno and Ryan 1986, Rosenbaum and Lister 2004].

Neogene magmatism promoted the development of geothermal systems since the late Miocene. The long lasting magmatic activity in the area [Serri et al. 1993, Dini et al. 2005] is also recorded by the occurrence of an exposed fossil geothermal system in eastern Elba Island [Dini et al. 2008, Mazzarini et al. 2011] as well as by the occurrence of the well known active Larderello-Travale geothermal field exploited for power production since 1911 [Gianelli and Ruggieri 2002, Dini et al. 2005, Bertini et al. 2006].

2.1. The Calamita hydrothermal system (CHS)

The CHS developed within a contact aureole about 6 Ma ago in eastern Elba Island at the Calamita Peninsula (Dini et al. [2008], Mazzarini et al. [2011]; Figure 2a); it is an example of high temperature hydrothemal system consisting of tourmaline-filled veins hosted within the Calamita Schist Fm., an early Carboniferous terrigeneous sequence, involved in alpine deformation and overprinted by contact metamorphism at about 6 Ma [Mazzarini et al. 2011, Musumeci et al. 2011]. Fluids generated from boron-rich intrusions (Porto Azzurro pluton) and circulated trough fractures generated by hydro-fracturing and deformation [Dini et al. 2008, Mazzarini et al. 2011]. CHS developed at depth less than 7-6 km as suggested by thermobaric conditions of contact metamorphism (P_{max} < 0.18-0.2 GPa) in host rock [Duranti et al. 1992, Mazzarini and Musumeci 2008].

Tourmaline-rich veins are widespread on the eastern side of Calamita peninsula from north of Calanova to south of Punta Bianca (Figure 2a). The veins are filled by fine- to very fine-grained black (schorl-dravite) and/or brownish (uvite) tormaline and rare quartz. Their composition records the circulation of magmatic, boron-rich hydrothermal fluids that partly interacted with the host rocks [Dini et al. 2008]. Preliminary analyses on fluid inclusion hosted in quartz reveal that the fluid was characterized by very-high salinity (up 44 wt.% NaCl equivalent), in agreement with its magmatic nature, and temperature ≥ 330-360°C. Tourmaline veins were emplaced into high-grade hornfels of the Calamita Schist, and are characterized by an uneven spatial distribution from Barbarossa to the north and Punta Bianca to the south, with the highest density occurring in the Cala Stagnone e Capo Calvo area (Figure 2a). Two vein sets (A veins and B veins) have been defined on the basis of their attitude as well as infilling material (Figure 3a), their relative abutting relationships indicate coeval emplacement [Dini et al. 2008, Mazzarini et al. 2011]. The A-set (207 veins) comprises steeply-dipping veins that are well clustered around N–S to NNW–SSE strike directions. This set is composed only of black tourmaline (schorl-dravite) veins [Dini et al. 2008]. The B-set (98 veins) is characterized by gentle to moderate dips and a dispersed strike distribution around a dominant NW–SE trend and a minor E–W trend. B veins are filled by black tourmaline (schorl-dravite) and by brownish tourmaline (uvite) [Dini et al. 2008].

2.2. The Scarlino hydrothermal system (SHS)

The SHS, hosted within late Oligocene sandstone of the Macigno Fm. (foredeep deposits of the Tuscan Nappe), in southern Tuscany, has been examined along a coastal section at Cala Martina and in an abandoned quarry, Cava Botrona, few kilometres inland (Figure 2b; Mazzarini and Isola [2007], Mazzarini et al. [2010]). The veins in SHS are a well-documented example of early Pliocene – late Pleistocene relatively low temperature hydrothermal system consisting of calcite-rich veins that exploited an inherited fracture network within a monotonous sandstone sequence [Mazzarini and Isola 2007, Mazzarini et al. 2010]. Hydrothermal fluids were formation waters at temperature of 160-260°C, at maximum depth of 5 km as derived by both structural and fluid inclusion analyses [Mazzarini and Isola 2007, Mazzarini et al. 2010].

In the SHS, the main trends of veins are NE–SW, E–W, N–S and NW–SE (Figure 3b). At Cala Martina attitude of 724 veins have been measured, and at Cava Botrona up to 546 measurements have been collected. Most of the measured veins are steeply dipping with only about 10% of the measured veins dips less than 40°. Shallow dipping veins are generally present in siltstones and in laminated fine-grained sandstones; they are concordant to para-concordant with the sandstones sedimentary bedding [Mazzarini et al. 2010].

3. Transmissivity

Transmissivity (T) records the fluid movement through rocks and for fractures it is directly related to the fracture aperture obeying to the cubic law [e.g. Witherspoon et al. 1980, Surrette and Allen 2008]. According to the cubic law the fracture transmissivity (T) is thus defined as:

$$T = \alpha b^3 \qquad (1)$$

where $\alpha = \rho g / 12\,\mu$ (ρ and μ being the fluid's density and viscosity, respectively, and g the gravity), and it is supposed to be a fluid property and considered, in first approximation, constant. In this study we substitute the fracture hydraulic aperture (b) with the vein's thickness (w).

The hydraulic transmissivity of an array of veins can be modeled as the sum of the contributions of all the veins of the array [e.g. Bear 1993], thus the array transmissivity (T_{tot}) is $T_{tot} = \sum_i^n T_i$, where $T_i = \alpha w_i^3$ is the transmissivity of the n_i veins in the interval of thickness Δx_i with average aperture w_i. The mean aperture of the veins' population is derived from the sampled veins

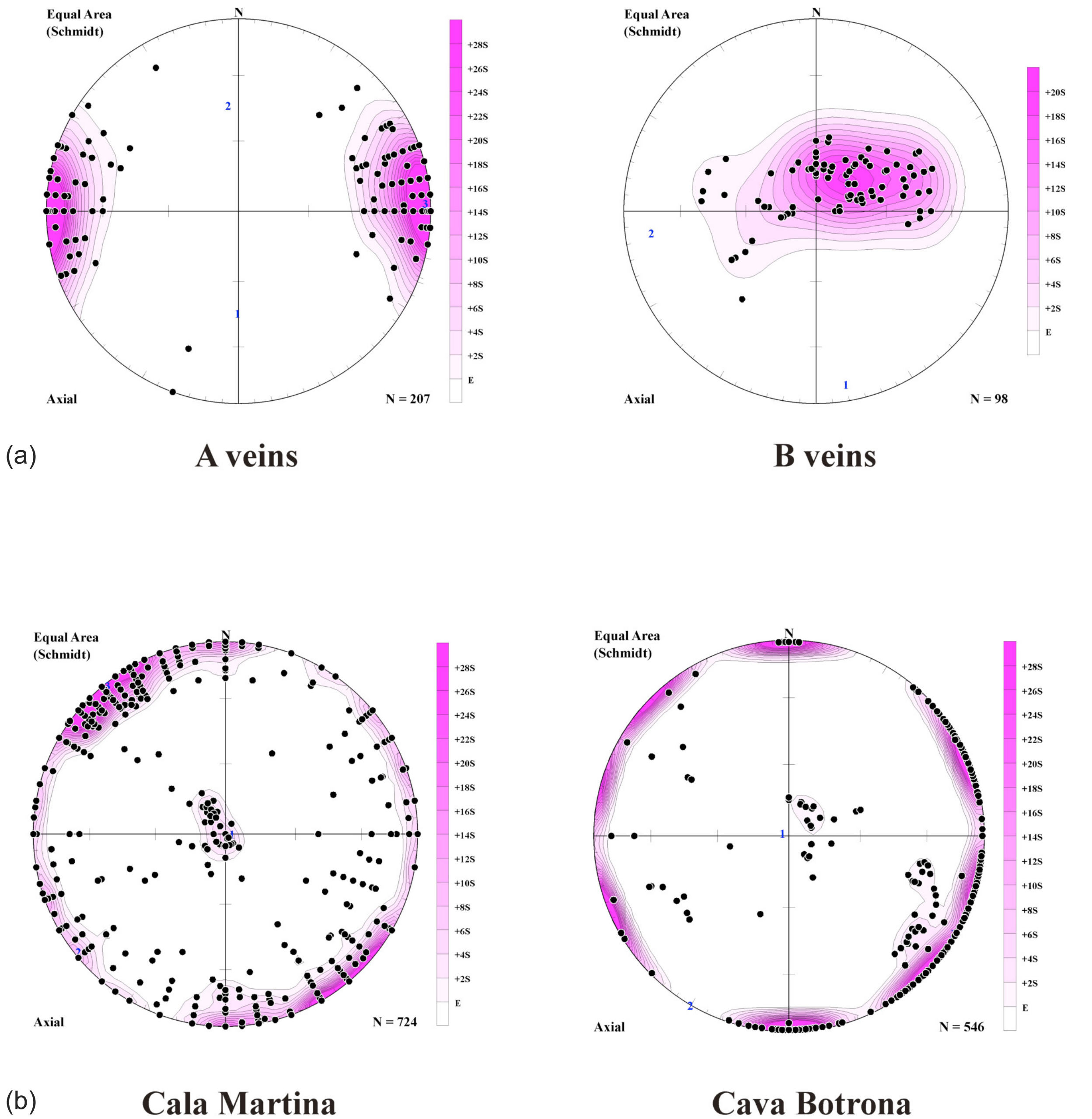

Figure 3. (a) Lower hemisphere stereo plots of pole to veins for the CHS hydrothermal systems. (b) Lower hemisphere stereo plots of pole to veins for the SHS hydrothermal systems. Contouring is done by the number of counts (E) expressed as multiples of standard deviation (S).

thickness and the vein network transmissivity can be assumed to be proportional to w^3:

$$T_{tot} \approx w^3 \tag{2}$$

where w^3 is the average cubic aperture of the vein systems.

It is here suggested that the analysis of veins' thickness distribution may provide clues on the system transmissivity without information on properties of circulating fluids.

4. Veins thickness distribution

Geometric features of veins, such as thickness and spacing, are characterized by scale invariance [e.g. Roberts et al. 1999, Gillespie et al. 1999, Bonnet et al. 2001] and are analyzed in terms of their cumulative distribution. The thickness distribution of veins has been described by power-law or negative exponential [e.g. Johnston and McCaffrey 1996, Gillespie et al. 1999, Loriga 1999, Roberts et al. 1999]. Power-law distribution is defined as:

$$N(> w) = cw^{-D} \tag{3a}$$

where c is a normalization constant, w is the vein thickness and D is the power law exponent. Negative exponential distribution is:

$$N(> w) = \beta e^{-aw} \tag{3b}$$

where β and a are the distribution parameters.

Veins thickness distribution can be used to infer the mechanism for the vein growth [e.g. Clark et al. 1995, Roberts et al. 1999]. Clark et al. [1995] proposed a constant nucleation of veins with a time-averaged growth rate proportional to thickness characterized by a power-law distribution of veins thickness. A negative exponential distribution for the vein thickness is expected for a constant veins growth rate. Monecke et al. [2001] assumed that the scaling exponent $a(\alpha/\gamma)$ is function of nucleation (α) and growth rates (γ). High nucleation rates lead to high scaling exponent, i.e. distribution dominated by thin veins, whereas very high growth rates produce low scaling exponent that is a distribution dominated by thick veins.

The following points should be considered when determining distribution parameters: (1) the error associated with the resolution limit of measurement (truncation), and (2) the error resulting from values of the measured feature extending beyond the sampling window (censoring). The effect of truncation is to underestimate the contributions of measurements (e.g., thickness) below the resolution of the acquisition method (for example, veins with thickness less than 0.5 mm). The effect of censoring is to underestimate measurements extending beyond the sampling window (e.g., spacing greater than a few tens of meters). Comparison of theoretical maximum values of the distribution (w_{max}) with the maximum sampled value can thus give an indication of the influence of censoring and truncation; the higher the difference between these values, the higher is the influence of under sampling.

The theoretical maximum thickness could be derived by imposing $N(>w)=1$ and solving for w in Equation (3).

Veins' thickness has been measured in CHS and SHS at several distinct sites, along transects a few hundred of meters apart, paying attention to sampling veins only once at each site.

The thickness of the veins (w) is measured normal to the vein walls and the largest exposed thickness is recorded. The simple arithmetic average thickness (w_a) computed for the sampled thicknesses is $w_a = \Sigma_i w_i / N$, where N is the number of samples. For each data set the maximum (TM) and minimum (tm) observed vein thicknesses are also recorded. We assume that veins in the analyzed systems are essentially non-stratabound veins on the basis of field observation and because they formed in the 3-6 km depth range [Mazzarini and Isola 2007, Mazzarini et al. 2010, 2011].

The cumulative distribution of the thickness for natural veins systems is defined between a lower and an upper limit (the minimum value $tmin$ and the maximum value $Tmax$), and can be generally defined as:

$$N(w) = \int_{w}^{T\max} g(x)dx \tag{4}$$

where $N(w)$ is the number of veins with thickness greater than w, and $Tmax$ is the maximum of the thickness population, and $g(w)\delta w$ is the number of veins in the interval $[w, w+\delta w]$ and $g(w) = -N'(w)$. In terms of cumulative distribution $N(w)$ the number of veins in the interval $[w, w+\delta w]$ is $-N'(w)\delta w$ and the average vein thickness derived from the cumulative thickness distributions and referred to the thickness interval observed in the field (tm, TM) is:

$$\bar{w} = \frac{-\int_{tm}^{TM} x\dot{N}(x)dx}{N(tm) - N(TM)} \tag{5}$$

For power-law distribution (Equation 3a) the first derivative is $N'(w) = -cDw^{-(D+1)}$, whereas for a negative exponential distribution (Equation 3b) it is $N'(w) = -\beta a e^{-aw}$.

The average vein thickness for a given distribution is thus computed by solving Equation (5); for a power-law distribution is:

$$\bar{w}_p = \frac{-\int_{tm}^{TM} -cDx^{-(1+D)}x\,dx}{c(tm^{-D} - TM^{-D})} = \frac{D(TM^{(1-D)} - tm^{(1-D)})}{(1-D)(tm^{-D} - TM^{-D})} \tag{6a}$$

where c and D are the normalization constant and the power law exponent, respectively.

For a negative exponential distribution the average vein thickness is:

$$\bar{w}_{ne} = \frac{-\int_{tm}^{TM} -\beta a e^{-ax}x\,dx}{\beta(e^{-atm} - e^{-aTM})} = \frac{e^{-atm}\left(tm + \frac{1}{a}\right) - e^{-aTM}\left(TM + \frac{1}{a}\right)}{(e^{-atm} - e^{-aTM})} \tag{6b}$$

where β and a are the distribution parameters, respectively.

Similarly, Mazzarini et al. [2010] derived the average cubic thickness for a power-law distribution:

$$\bar{w}_p^3 = \frac{D(TM^{(3-D)} - tm^{(3-D)})}{(3-D)(tm^{-D} - TM^{-D})} \tag{7a}$$

and

$$\bar{w}_p^3 = \frac{\left[e^{-ax}(a^2x^3 + 3ax^2 + 6x - 6)\right]_{tm}^{TM}}{(3-D)(tm^{-D} - TM^{-D})} \tag{7b}$$

for negative exponential distribution.

5. Results

Based on the analysis of the thickness distribution of veins in CHS and SHS, we estimated the veins transmissivity in order to investigate the conductance of fractured rocks at the time and depth of veins formation.

Several artifacts occur when fracture aperture data are analyzed. In order to overcome these artifacts data normalization and scaling procedure have been proposed [e.g., Ortega et al. 2006, Guerriero 2012]. Here we propose a rough and fast method to analyze veins thickness distribution. The power law is computed within the size range defined in the thickness range where the goodness of fit (R^2 in Table 1) is high and it is greater than that of exponential distribution. We assume that measured vein thicknesses are a sampling of the true thickness population. As described by Mazzarini et al. [2011], when the theoretical maximum values of distributions for all the analyzed data sets are very close to the empirical maximum (i.e., the observed maximum thicknesses measured in the field), the actual thickness distribution of the veins is well sampled and censoring artifacts are reduced (Table 2).

In the high temperature hydrothermal system (CHS), 282 veins thicknesses were measured; 216 from the A set and 54 from the B set (Table 1; Figure 4a,b). Overall, vein thicknesses have a mean of 1.8 cm. A-set veins have thicknesses varying from 0.1 to 16.5 cm with an average of 1.5 cm, and B-set veins have thicknesses ranging from 0.05 to 25 cm with an average of 2.7 cm.

Thickness distributions for A and B vein sets are well described by power-law distributions (Figure 5a). A-set veins has $D \sim 2.04$ in the 2.4-16 cm size range, B-set veins has $D \sim 1.35$ in the 2.2-24 cm size range; finally, all the veins have $D \sim 1.85$ in the 1.8-24 cm size range (Table 1).

In the low temperature hydrothermal system (SHS), at the Cala Martina, 609 vein thicknesses have been measured and 246 measurements at the Cava Botrona (Table 1; Figure 4c,d). At Cala Martina (CM) vein thickness has an average of 0.357 cm in the 0.05-7.0 cm range. The maximum thickness of 7 cm observed in the field is related to a hydro fracture [Mazzarini et al. 2010].

Veins' thickness at Cava Botrona (CB) has an average of 0.234 cm in the 0.05-1.36 cm range (Table 1). At Cala Martina a power-law vein thickness distribution is

	Data set	n	$n(w)$	R^2	s.r. (cm)	w_a (cm)	σ (cm)	$TM - tm$ (cm)
CHS	all	282	$376.23w^{-1.8484}$	0.9612	1.8-24	1.8	2.8	25.0 – 0.05
	A	216	$320.24w^{-2.0444}$	0.9787	2.4-16	1.5	2.2	16.5 – 0.1
	B	54	$63.933w^{-1.3511}$	0.9366	2.2-24	2.7	4.4	25.0 – 0.05
SHS	CB	246	$432.56e^{-0.6943w}$	0.9921	0.05-0.82	0.234	0.158	1.36 – 0.05
	CM	609	$2225.3w^{-1.8835}$	0.9762	0.25-2.50	0.357	0.484	3.50 – 0.05

Table 1. Distribution and statistics of veins in the studied hydrothermal systems. n: sample number; $n(w)$: cumulative distribution, number of veins with width larger than w; R^2: goodness of fit; s.r.: size range of distribution; w_a: arithmetic average estimation of veins thickness of samples; σ: standard deviation; TM, tm: maximum and minimum vein thicknesses from field data, respectively.

Site	Data set	n	w (mm)	TM (cm)	w_{max} (cm)	w^3 (m^3)	Distribution
CHS	all	282	1.1	25.0	24.0	2.6×10^{-7}	p.l.
	A	216	1.9	16.5	16.8	2.8×10^{-7}	p.l.
	B	54	1.7	25.0	21.7	2.9×10^{-6}	p.l.
SHS	CM	609	1.1	7.0	6.0	0.5×10^{-7}	p.l.
	CB	246	1.9	1.36	0.9	3.0×10^{-5}	n.e.

Table 2. Contribution of veins to the transmissivity (cubic law). n: number of veins; w: average thickness derived by the thickness distribution; w_{max}: theoretical maximum thickness; w^3: average cubic thickness of vein network by Equations (7); p.l.: power law distribution; n.e.: negative exponential distribution.

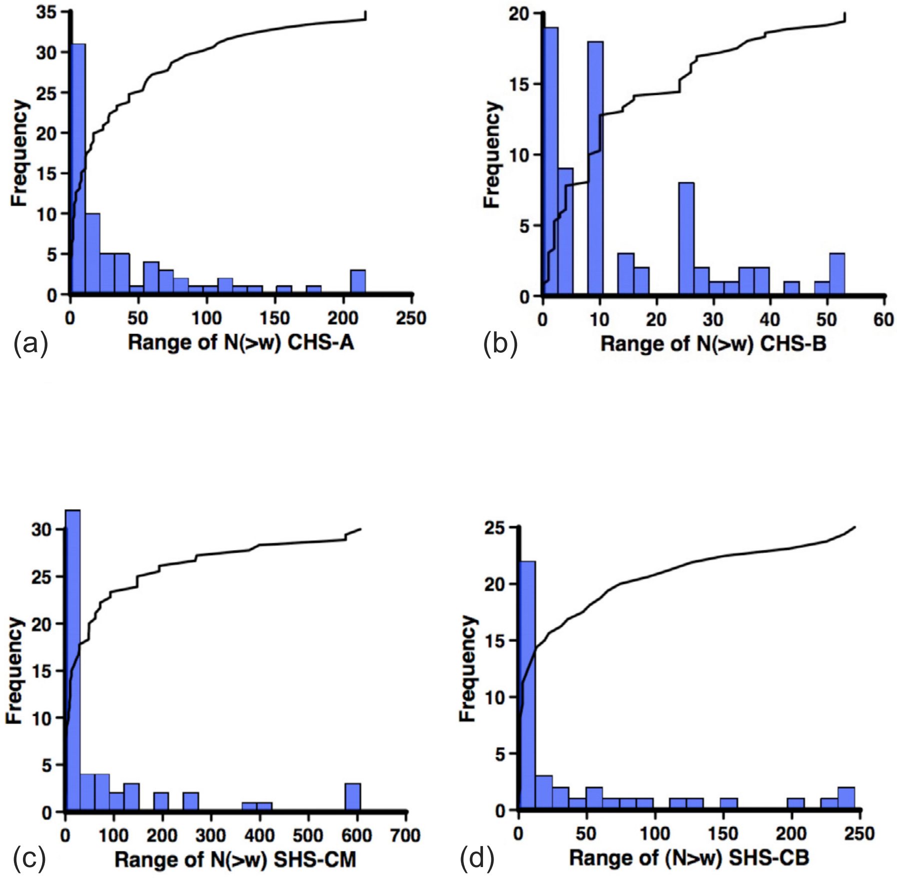

Figure 4. Histograms and cumulative curves (black solid lines) for the measured vein thickness. (a) Thickness distribution for CHS-A. (b) Thickness distribution for CHS-B. (c) Thickness distribution for SHS-CM. (d) Thickness distribution for SHS-CB.

clearly defined with $D \sim 1.88$ in the 0.25-2.5 cm size range, whereas at Cava Botrona a negative exponential thickness distribution with $a \sim 0.69$ in the 0.05-8.2 cm size range (Table 1) best fits the observed data (Figure 5b).

Comparing Table 1 and Table 2, it is clear that the average vein thicknesses derived from the population distributions (i.e. Equations 6) differ sensibly from the simple arithmetic average thickness (w_a). According to Equations (7) in Table 2 the average cubic thickness for all the data sets are listed.

6. Discussion

The transmissivity of the vein networks in the studied hydrothermal systems, according to Equation (1) depend on fluid characteristic parameter (α) that is function of fluid density and dynamic viscosity. The dynamic viscosity of aqueous fluids depends on fluid temperature and may drastically change as fluid is close to the critical point [e.g. Watson et al. 1980]. Anyway, at a specific time, the parameter α could be assumed constant, and we could use the thickness estimation to infer transmissivity characteristics for the studied hydrothermal systems.

As stated above, veins thickness is often characterized by scale invariance [e.g. Johnston and McCaffrey 1996, Gillespie et al. 1999], this implies that a simple arithmetic average of the sampled population may give erroneous estimation of the mean thickness. By comparison of Tables 1 and 2, we observe that the arithmetic average of observations clearly overestimates the true average thickness as derived by distributions (Equations 6a,b).

The high temperature hydrothermal system (CHS) shows ubiquitous power-law distributions for all the studied data sets (Table 1), using the value of w^3 as a proxy for the vein transmissivity (transmissivity is proportional to the cubic power of thickness) it is apparent that the lower the D exponent of the distribution the higher the transmissivity (Table 2); in fact A-veins with $D \sim 2.0$ has transmissivity (i.e. $\sim w^3$) one order lower than transmissivity of B-veins with $D \sim 1.4$ (Table 2). High D exponent indicates distributions dominated by small size elements (thin veins in this case), the lower the D exponent the more the thick veins. These latter mainly control the overall transmissivity for the cubic law (see Equation 1). The transmissivity of the whole measured veins is less than the sum of the two vein systems transmissivity (A+B > all, in Table 2), indicating that the two vein sets behaved as independent fluids pathways at the time of vein formation.

In the low temperature hydrothermal system (SHS), veins thickness shows power-law (Cala Martina,

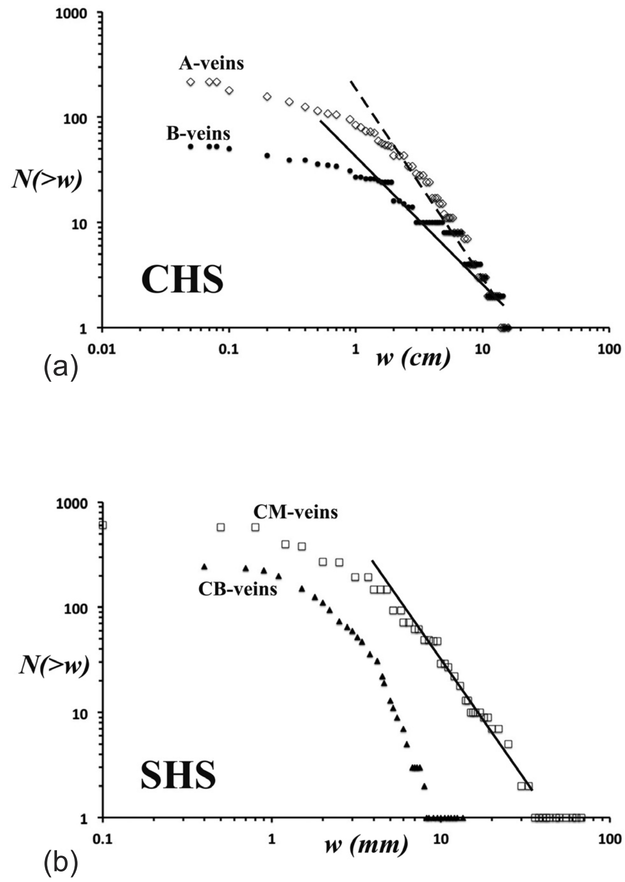

Figure 5. Log-log plots for the veins' thickness distribution for the data sets in CHS and SHS (see also Table 1).

CM) and negative exponential (Cava Botrona, CB) distributions (Table 1).

The w^3 value, a proxy of the overall transmissivity (Table 2), of the Cava Botrona site (negative exponential distribution) is almost three orders of magnitude higher than that of the Cala Martina site (power law distribution). The high scaling exponent associated to the CM data set ($D \sim 1.88$, Table 1) indicates that at CM the system is mainly controlled by thin veins, whereas, the CB data set, characterised by negative exponential distribution ($a \sim 0.69$) is less sensitive to thin veins (Table 1). This holds when power law distribution with exponent close to 2 is observed, being it characterised by numerous thin veins that account for only a small amount of the total fluid discharge.

Our results suggest that enhanced permeability driven by tectonics (extension fractures) controls fluid circulation across large distances. This control occurs especially in uppermost brittle crust. The analysis of thickness distribution may thus provide information on the hydraulic properties of the actual fracture network at the time of vein formation. We observed that in upper brittle crust, whatever the fluid genesis and temperature (high temperature magmatic/ metamorphic fluids, or low temperature connate waters), the exploitation of a fracture network, recorded as a veins, provides an efficient mass transfer in hydrothermal systems. Distribution of thickness in hydrothermal veins represent a good proxy to image the fluid circulation at depth, and may provide conceptual framework for numerical modeling of fluid circulation in active geothermal/ hydrothermal systems.

References

Bear, J. (1993). Modeling flow and contaminant transport in fractured rocks, In: J. Bear, C.F. Tsang and G. De Marsily (eds.), Flow and contaminant transport in fractured rock, Academic Press, 1-37.

Bertini, G., M. Casini, G. Gianelli and E. Pandeli (2006). Geological structure of a long-living geothermal system, Larderello, Italy, Terra Nova, 18, 163-169.

Boccaletti, M., P. Elter and G. Guazzone (1971). Plate tectonics models for the development of Western Alps and Northern Apennines, Nature, 234, 108-111.

Bonnet, E., O. Bour, N. Odling, I. Main, B. Berkowitz, P. Davy and P. Cowie (2001). Scaling of fracture systems in geological media, Rev. Geophys., 39, 347-383.

Bons, P.D. (2001). The formation of large quartz veins by rapid ascent of fluids in mobile hydrofractures, Tectonophysics, 336, 1-17.

Clark, M.B., S.L. Brantley and D.M. Fisher (1995). Power-law vein-thickness distribution and positive feedback in vein growth, Geology, 23, 975-978.

Cox, S.F., M.A. Knackstedt and J. Braun (2001). Principle of structural control on permeability and fluid flow in hydrothermal system, In: J. Richards and R. Tosdal (eds.), Deformation, Fluid Flow and Ore Deposits, Rev. Econ. Geol., 14, 1-24.

Cui, X., P.I. Nabelek and M. Liu (2001). Heat and fluid flow in contact metamorphic aureoles with layered and transient permeability, with application to the Notch Peak aureole, Utah, J. Geophys. Res., 106, B4, 6477-6491.

Darcel, C., O. Bour, P. Davy and J.R. de Dreuzy (2003). Connectivity properties of two-dimensional fracture networks with stochastic fractal correlation, Water Resour. Res., 39, 1272; doi:10.1029/2002WR001628.

Dini, A., G. Gianelli, M. Puxeddu and G. Ruggieri (2005). Origin and evolution of Pliocene-Pleistocene granites from the Larderello geothermal field (Tuscan Magmatic Province, Italy), Lithos, 81, 1-31.

Dini, A., F. Mazzarini, G. Musumeci and S. Rocchi (2008). Multiple hydro-fracturing by boron-rich fluids in the late Miocene contact aureole of eastern Elba Island (Tuscany, Italy), Terra Nova, 20, 318-326.

Duranti, S., R. Palmeri, P. Pertusati and C.A. Ricci (1992). Geological evolution and metamorphic petrology of the basal sequence of eastern Elba (complex II), Acta

Vulcanologica, 2, 213-229.

Gianelli, G., and G. Ruggieri (2002). Evidence of a contact metamorphic aureole with high-temperature metasomatism in the deepest part of the active geothermal field of Larderello, Italy, Geothermics, 31, 443-474.

Gillespie, P.A., J.D. Johnston, M.A. Loriga, K.J.W. McCaffrey, J.J. Walsh and J. Watterson (1999). Influence of layering on vein systematics in line samples, In: K.J.W. McCaffrey, L. Lonergan and J.J. Wilkinson (eds.), Fractures, Fluid Flow and Mineralization, Geological Society, London, Special Publications, 155, 35-56.

Guerriero, V., S. Vitale, S. Ciarcia and S. Mazzoli (2011). Improved statistical multi-scale analysis of fractured reservoir analogues, Tectonophysics, 504, 14-24; doi:10.1016/j.tecto.2011.01.003.

Guerriero, V. (2012). Power Law Distribution: Method of Multi-scale Inferential Statistics, J. Mod. Math. Frontier, 1, 21-28.

Guerriero, V., S. Mazzoli, A. Iannace, S. Vitale, A. Carravetta and C. Strauss (2013). A permeability model for naturally fractured carbonate reservoirs, Mar. Petrol. Geol., 40, 115-134; doi:10.1016/j.marpetgeo.2012.11.002.

Hanson, R.B. (1995). The hydrodynamics of contact metamorphism, Geol. Soc. Am. Bull., 107 (5), 595-611.

Hsieh, P.A. (1998). Scale effects in fluid flow through fractured geological media, In: G. Sposito (ed.), Scale Dependence and Scale Invariance in Hydrogeology, Cambridge Univ. Press, 335-353.

Johnston, J.D., and K.J.W. McCaffrey (1996). Fractal geometries of vein systems and the variation of scaling relationships with mechanism, J. Struct. Geol., 18, 349-358.

Loriga, M.A. (1999). Scaling systematics of vein size: an example from the Guanajuato mining district (Central Mexico), In: K.J.W. Mc Caffrey, L. Lonergan, L. and J.J. Wilkinson (eds.), Fractures, Fluid Flow and Mineralization, Geological Society, London, Special Publications, 155, 57-67.

Malinverno, A., and W.B.F. Ryan (1986). Extension on the Tyrrhenian sea and shortening in the Apennines as result of arc migration driven by sinking of the lithosphere, Tectonics, 5, 227-245.

Mazzarini, F., and I. Isola (2007). Hydraulic connection and fluid overpressure in upper crustal rocks: evidence from geometry and spatial distribution of veins at Botrona quarry, southern Tuscany, Italy, J. Struct. Geol., 29, 1386-1399.

Mazzarini, F., and G. Musumeci (2008). Hydrofracturing related sill and dyke emplacement at shallow crustal level: the eastern Elba Dyke Complex, Italy, In: K. Thomson and N. Petford (eds.), Structure and Emplacement of High-Level Magmatic Systems, Geological Society, London, Special Publications, 302, 121-129.

Mazzarini, F., I. Isola, G. Ruggieri and C. Boschi (2010). Fluid circulation in the upper brittle crust: thickness distribution, hydraulic transmissivity fluid inclusion and isotopic data of veins hosted in the Oligocene sandstones of the Macigno Formation in southern Tuscany, Italy, Tectonophysics, 493, 118-138; doi:10.1016/j.tecto. 2010. 07.012.

Mazzarini, F., G. Musumeci and A.R. Cruden (2011). Vein development during folding in the upper brittle crust: The case of tourmaline-rich veins of eastern Elba Island, northern Tyrrhenian Sea, Italy, J. Struct. Geol., 33, 1509-1522; doi:10.1016/j.jsg.2011.07.001.

McCaffrey, K.J.W., and J.D. Johnstont (1996). Fractal analysis of a mineralised vein deposit: Curraghinalt gold deposit, County Tyrone, Mineralium Deposita, 31, 52-58.

Monecke, T., J.B Gemmell and J. Monecke (2001). Fractal distribution of veins in drill core from the Hellyer VHMS deposit, Australia: constraints on the origin and evolution of the mineralising system, Mineralium Deposita, 36, 173-188.

Musumeci, G., F. Mazzarini, M. Tiepolo and G. Di Vincenzo (2011). U-Pb and 40Ar-39Ar geochronology of Palaeozoic units in the northern Apennines: determining protolith age and alpine evolution using the Calamita Schist and Ortano Porphyroid, Geol. J., 46, 288-310; doi:10.1002/gj.1266.

Odling, N.E., P. Gillespie, B. Bourgine, C. Castaing, J.P. Chiles, N.P. Christensen, E. Fillion, A. Genter, C. Olsen, L. Thrane, R. Trice, E. Aarseth, J.J. Walsh and J. Watterson (1999). Variations in fracture system geometry and their implications for fluid flow in fractured hydrocarbon reservoirs, Petrol. Geosci., 5, 373-384.

Oliver, N.H.S. (1996). Review and classification of structural controls on fluid flow during regional metamorphism, J. Metamorph. Geol., 14, 477-492.

Ortega, O., R. Marrett and E. Laubach (2006). Scale-independent approach to fracture intensity and average spacing measurement, AAPG Bulletin, 90, 193-208

Roberts, S., D.J. Sanderson and P. Gumiel (1999). Fractal analysis and percolation properties of veins, In: K.J.W. McCaffrey, L. Lonergan and J.J. Wilkinson (eds.), Fractures, Fluid Flow and Mineralization, Geological Society, London, Special Publication, 155, 71-16.

Rosenbaum, G., and G.S. Lister (2004). Neogene and Quaternary rollback evolution of the Tyrrhenian Sea, the Apennines and the Sicilian Maghrebides, Tectonics, 23, TC1013; doi:10.1029/2003TC001518.

Rosenbaum, G., M. Gasparon, F.P. Lucente, A. Peccerillo and M.S. Miller (2008). Kinematics of slab tear during subduction and implications for Italian Magmatism, Tectonics, 27, TC2008; doi:10.1029/2007TC002143.

Serri, G., F. Innocenti and P. Manetti (1993). Geochemical and petrological evidence of the subduction of delaminated Adriatic continental lithosphere in the genesis of the Neogene–Quaternary magmatism of central Italy, Tectonophysics, 223, 117-147.

Surrette, M.J., and D.M. Allen (2008). Quantify heterogeneity in variably fractured sedimentary rock using a hydrostructural domain, Geol. Soc. Am. Bull., 120, 225-237.

Vermilye, J.M., and C.H. Scholz (1995). Relation between vein length and aperture, J. Struct. Geol., 17, 423-434.

Watson, J.T.R., R.S. Basu and J.V. Sengers (1980). An improved representative equation for the dynamic viscosity of water substance, J. Phys. Chem. Ref. Data, 9 (4), 1255-1290.

Witherspoon, P.A., J.S.Y. Wang, K. Iwai and J.E. Gale (1980). Validity of cubic law for fluid flow in a deformable rock fracture, Water Resour. Res., 16, 1016-1024.

*Corresponding author: Francesco Mazzarini,
Istituto Nazionale di Geofisica e Vulcanologia, Sezione di Pisa,
Pisa, Italy; email: mazzarini@pi.ingv.it.